Chapter 2

A Unified View of the Role of Electrostatic Interactions in Modulating the Gating of Cys-Loop Receptors

Reproduced in part from:
X.Xiu, A.P. Hanek, J. Wang, H.A. Lester, and D.A. Dougherty
J. Biol. Chem. **2005**, 280 (50), 41655-41666

2.1 Introduction

The Cys-loop superfamily of neurotransmitter-gated ion channels plays a prominent role in mediating fast synaptic transmission. Receptors for acetylcholine (nicotinic ACh receptor, nAChR), serotonin (5-HT_3 receptor), γ-aminobutyric acid (GABA, types A and C receptors), and glycine are known, and the receptors are classified as excitatory (cation-conducting; nAChR and 5-HT_3) or inhibitory (anion-conducting; GABA and glycine). Malfunctions in these receptors are responsible for a number of "channelopathies," and the receptors are targets of pharmaceutical efforts toward treatments for a wide range of neurological disorders, including Alzheimer's disease, Parkinson's disease, addiction, schizophrenia, and depression.[1,2] The receptors share a common architecture, are significantly homologous, and are known to have evolved from a single ancestral gene that coded for an ACh receptor.

The gating mechanism for the Cys-loop superfamily is one of the most challenging questions in molecular neuroscience. At issue is how the binding of a small molecule neurotransmitter can induce a structural change in a large, multisubunit, integral membrane protein sufficient to open (gate) a previously closed ion channel contained within the receptor.[3,4] All evidence indicates that the neurotransmitter-binding site is

quite remote (50–60 Å) from the channel gate, the region that blocks the channel when the neurotransmitter is absent and that must move to open the channel.

The quest for a gating mechanism has been greatly aided by several recent structural advances. First, crystal structures of the soluble acetylcholine-binding protein (AChBP),[5-7] which is homologous to the extracellular domain of the nAChR and, by extension, other members of the superfamily, provide a good sense of the layout of the agonist-binding site and its relationship to the rest of the receptor. Second, continued refinement of cryo-EM images of the *Torpedo* nAChR by Unwin and co-workers,[8-11] incorporating insights gained from the AChBP structure, has produced a full atomic scale model (Protein Data Bank code 2BG9) of the nAChR. It is important to appreciate that 2BG9, although heuristically quite valuable, is not a crystal structure of the nAChR. Rather, it is a model built from low resolution data and homology modeling. Nevertheless, it represents a substantial advance for the field, and all modern attempts to obtain molecular scale information on the structure and function of Cys-loop receptors must consider this as a starting point.

The full 2BG9 model of the nAChR[11] immediately suggested ways in which the agonist-binding site could couple to the transmembrane region and thus initiate gating. As summarized in Figure 2.1, loops 2, 7, and 9 from the AChBP structure are oriented toward the transmembrane region, and indeed, in 2BG9 these loops make contacts with parts of the transmembrane domain. Note that loop 7 is the eponymous Cys-loop. The transmembrane region consists of four α-helices per subunit, labeled M1–M4. It is accepted that M2 lines all or most of the channel. Helix M1 extends out of the transmembrane region toward the extracellular domain, creating a segment termed pre-

M1. Although M4 is somewhat separated from the rest of the protein in 2BG9, recent modeling studies produce a more compact structure in which M4 is more intimately involved.[12] In particular, the carboxy terminus of M4, a region we will term post-M4, can contact the extracellular domain. A key structure is the M2–M3 loop, a short connector between the two transmembrane helices. Topological considerations have long placed this loop at the interface between the transmembrane and extracellular domains. That expectation was resoundingly confirmed by Protein Data Bank code 2BG9, and many workers have anticipated that this loop could play an important role in gating. Indeed, recent work[13] has established that a key proline at the apex of the M2–M3 loop provides the conformational switch that gates the channel in the 5-HT_3 receptor.

Several groups have attempted to identify key interactions in the interface between the extracellular domain and the transmembrane domain, and we discuss some of these results below. This interface contains a number of charged residues, and most efforts have focused on these, attempting to find crucial electrostatic interactions that regulate gating. Specific hydrophobic interactions have also been proposed.[8,14] Several interacting pairs have been identified in various receptors,[15,16] and specific gating models based on critical electrostatic interactions have been proposed.[17-20] We note from the start, however, that *none* of the proposed interactions are conserved across the superfamily. We have been puzzled by the notion that in this closely related family of receptors, the mechanism of action of the essential function of the receptors seems to vary from system to system.

In the present work we argue that specific, pairwise electrostatic interactions at the interface between the transmembrane and extracellular domains are not critical to

gating. Rather, we argue it is the global charging of this region and the network of interacting ionic residues that are critical to receptor function. We present an overall analysis of charged interfacial residues in the Cys-loop superfamily, extensive mutagenesis studies of loop 2 residues involved in potential electrostatic interactions in the nAChR, and a reconsideration of previously published data on other receptors to support the model.

2.2 Results

2.2.1 Statistical analysis of the gating interface

For the purposes of discussion and analysis, we have defined a "gating interface" between the extracellular domain and the transmembrane domain. It is comprised of the following six segments: three from the extracellular domain (all or parts of loops 2, 7, and 9) and three from the transmembrane domain (pre-M1, M2–M3, and post-M4). The precise residues considered are given in Table 2.1. Unless otherwise noted, we will use the residue numbering system accepted for the nAChR α_1 subunit. The selection criterion for the gating interface was geometric; only residues that could reasonably be considered to experience a meaningful electrostatic interaction with another component of the gating interface were included. Because of the low resolution of the nAChR structure and the further uncertainty introduced by extrapolating to other Cys-loop receptors, precise distance constraints were not applied. Rather, as illustrated in Figure 2.1, we chose a contiguous band of residues in the region where the extracellular and transmembrane domains meet. Some leeway must be given in selecting possible interactions, as residues that are not in direct contact in 2BG9 could become so on transit from the closed state to the open state or when considering another receptor. Extending

the definition further out from the interface did not significantly impact the analysis. We will refer to the extracellular component (from loops 2, 7, and 9) and the transmembrane component (from pre-M1, M2–M3, and post-M4) when discussing the gating interface.

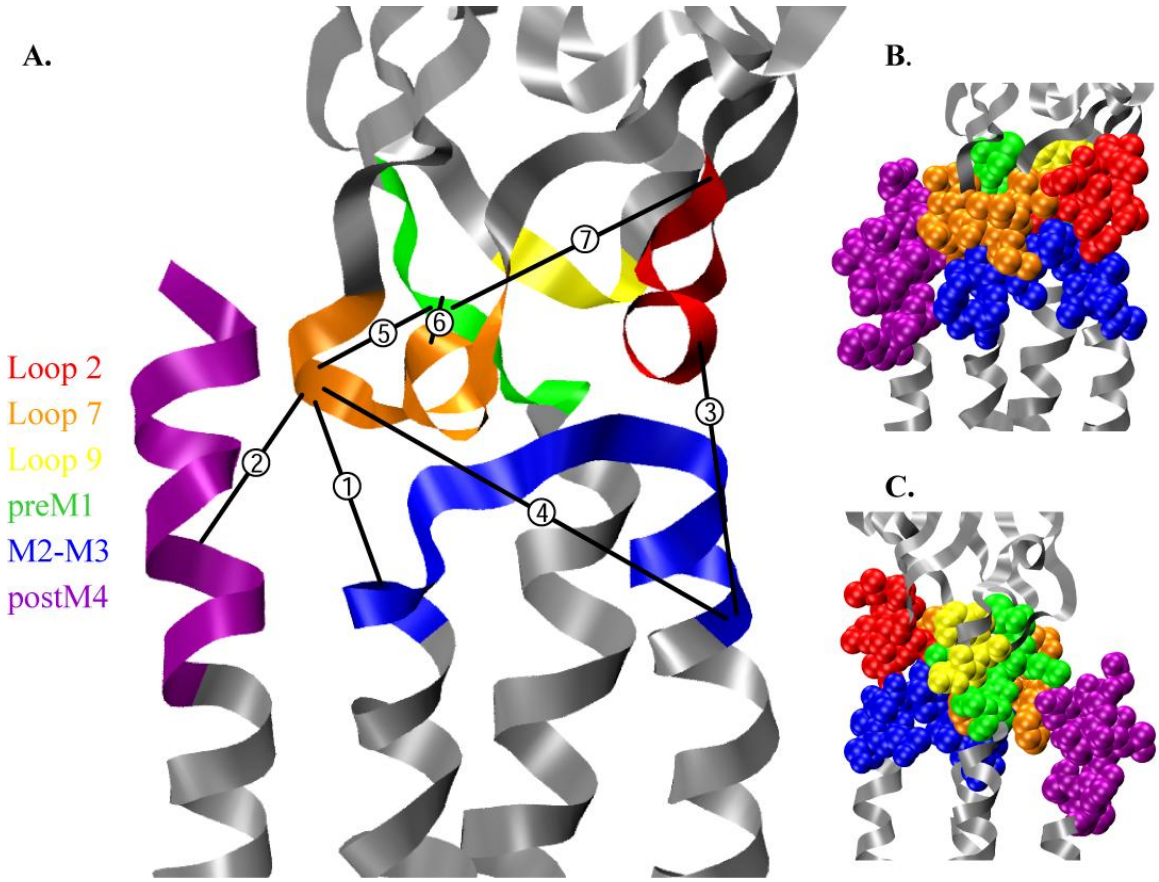

Figure 2.1 Views of the gating interface. Structure is the full model of an α subunit of the *Torpedo* nAChR developed by Unwin[11] (Protein Data Bank code 2BG9). Regions of the gating interface, as defined in text, are color-coded. **A**, ribbon diagram, also including pairwise interactions from various studies that have been proposed to contribute to the gating mechanism. Even though they are from different receptors and could be important in different states of the receptor, they are mapped onto the *Torpedo* structure to provide some sense of relative spatial relationships. Distances range from ~6 to ~20 Å. Interactions are as follows: *1*, D138 to K276 of muscle nAChR α_1 subunit ; *2*, D138 to R429 of muscle nAChR α_1 subunit; *3*, D57 to K279 of $GABA_A$ α_1 subunit; *4*, D149 to K279 of $GABA_A$ α_1 subunit; *5*, K215 to D146 of $GABA_A$ β_2 subunit; *6*, K215 to D139 of $GABA_A$ β_2 subunit; and *7*, K215 to D56 of $GABA_A$ β_2 subunit. **B**, same view as **A** with gating interface residues in space filling. **C**, view in B rotated 180° around vertical axis.

To search for patterns of charged residues, we considered the sequences of 124 subunits from the Cys-loop superfamily, 74 cationic and 50 anionic channel subunits (data not shown). Table 2.1 shows 22 representative subunits, 11 cationic (excitatory)

channels and 11 anionic (inhibitory) channels, and also serves to define the various segments. Table 2.2 summarizes the analysis of the full collection of the 124 subunits. Shown for each segment of the interface are the number of cationic residues (Lys and Arg), the number of anionic residues (Asp and Glu), the net charge (Z), and the number of charged residues (N).

Table 2.1 Selected sequences in the gating interface, highlighting cationic (blue) and anionic (red) residues

	Loop 2	Loop 7	L9	Pre-M1	M2-M3 Linker	Post-M4
Tor α	DEVNQI	IIVTHFPFDQ	EW	MQIRP	STSSAVPLIGKY	FAGRLIELSQEG
Tor β	NEKIEE	IKVMYFPFDW	QW	IQRKP	ETSLSVPIIIRY	FLDASHNVPPDN
Tor δ	NEKEEA	IAVTYFPFDW	EW	IQRKP	ETSLNVPLIGKY	FLTGHFNQVPEF
Tor γ	KETDET	INVLYFPFDW	EW	IRRKP	ETALAVPLIGKY	FVMGNFNHPPAK
nACh α_1	DEVNQI	IIVTHFPFDE	EW	MQRLP	STSSAVPLIGKY	FAGRLIELHQQG
nACh β_1	NEKDEE	IQVTYFPFDW	QW	IRRKP	ETSLAVPIIIKY	FLDATYHLPPPE
nACh δ	NEREEA	ISVTYFPFDW	EW	IQRKP	ETSQAVPLISKY	FLMAHYNQVPDL
nACh γ	KEVEET	ISVTYFPFDW	EW	IRRKP	ATSMAIPLVGKF	FLQGVYNQPPLQ
nACh α_4	DEKNQM	IDVTFFPFDQ	EW	IRRLP	STSLVIPLIGEY	FLPP--WLAGMI
nACh α_7	DEKNQV	IDVRWFPFDV	EW	MRRRT	ATSDSVPLIAQY	LMSAPNFVEAVS
5HT$_3$A	DEKNQV	LDIYNFPFDV	EW	IRRRP	ATAIGTPLIGVY	VMLWSIWQYA--
GABA α_1	SDHDME	MHLEDFPMDA	QY	LKRKI	KVAYATAM-DWF	LNREPQLKAPTP
GABA α_2	SDTDME	MHLEDFPMDA	QY	LKRKI	KVAYATAM-DWF	LNREPVLGVSP-
GABA α_3	SDTDME	MHLEDFPMDV	QY	LKRKI	KVAYATAM-DWF	VNRESAIKGMIR
GABA α_4	SDVDME	MRLVDFPMDG	QY	LKRKM	KVSYLTAM-DWF	LSKDTMEKSESL
GABA α_5	SDTEME	MQLEDFPMDA	QY	LKRKI	KVAYATAM-DWF	LNREPVIKGAAS
GABA α_6	SDVEME	MRLVNFPMDG	QY	LQRKM	KVAYATAM-DWF	LSKDTMEVSSSV
GABA β_1	SEVNMD	MDLRRYPLDE	QF	LKRNI	KIPY-VKAIDIY	VN----------
GABA β_2	SEVNMD	MDLRRYPLDE	QF	LKRNI	KIPY-VKAIDIY	VN----------
GABA β_3	SEVNMD	MDLRRYPLDE	QF	LKRNI	KIPY-VKAIDIY	VN----------
Gly α_1	AETTMD	MDLKNFPMDV	QF	LERQM	KVSY-VKAIDIW	KIVRREDVHNQ-
Gly α_2	TETTMD	MDLKNFPMDV	QF	LERQM	KVSY-VKAIDIW	KIVRHEDVHKK-
	44 49	130 139	175	207211	266 277	426

The abbreviations used are as follows: Tor, nAChR from *Torpedo californica*; nACh, nicotinic ACh receptor; 5-HT$_3$A, 5-HT$_3$ receptor, type A. All sequences were from human receptors except Tor and nACh α_1, β_1, δ, γ, which were from mouse muscle.

Although there is some variation, the typical gating interface contains 47 residues: 18 in the extracellular component and 29 in the transmembrane component. On average, 11.1 or 24% of these residues are charged. This is not significantly different from expectation based on the overall frequencies of occurrence of Asp, Glu, Arg, and Lys in

proteins (July, 2004, Swiss Protein Database). Most of the residues of the gating interface are or can be easily imagined to be water-exposed to some extent; therefore, this global result is not surprising. Of the ~11 charged residues found in the gating interface, only two are universally conserved, Asp-138 and Arg-209. So, although all Cys-loop receptors have a large number of ionic residues in the gating interface, their locations and absolute charges are variable.

Table 2.2 Charge characteristics of the gating interface

	+	-	Z	N
Loop 2	0.5	2.3	-1.8	2.8
Loop 7	0.4	1.9	-1.5	2.4
Loop 9	0.0	0.5	-0.5	0.5
Pre-M1	2.3	0.1	2.2	2.3
M2-M3	1.0	0.8	0.2	1.8
Post-M4	0.6	0.7	-0.1	1.3
Extracellular	0.9	4.8	-3.9	5.7
Transmembrane	3.9	1.6	2.3	5.5
Gating Interface	4.8	6.4	-1.6	11.1

The abbreviations used are as follows: + indicates number of cationic residues (K and R); - indicates number of anionic residues (D and E); Z indicates overall charge; and N indicates the number of ionic residues.

Although the two components of the gating interface do not have the same number of amino acids, the total number of charges is essentially the same (5.7 versus 5.5) for the two. There is, however, a dramatic difference in the net charge of the two components. The extracellular component has an overall negative charge, averaging -3.9 over the 124 subunits considered. The transmembrane component has an overall positive charge, averaging +2.3. Thus, there is a *global* electrostatic attraction in the interface, holding together the extracellular component and the transmembrane component. This interfacial electrostatic interaction is not created by simply putting anions in the extracellular component and cations in the transmembrane component; typically, there

are one cationic and five anionic side chains in the extracellular component but four cationic and two anionic side chains in the transmembrane component. We propose that it is the balance among all these charges that controls receptor function. With all these charges packed into a fairly compact space, we felt it more reasonable to consider a network of electrostatic interactions, rather than emphasizing any particular charged pair, as discussed below.

There is variability in the charging pattern of the gating interface. Considering only $GABA_A$ subunits, α_1 shows Z = -6 in the extracellular component and Z = +4 in the transmembrane component. In contrast, the α_4 subunit shows Z = - 4 in the extracellular component and Z = +2 in the transmembrane component. Despite the smaller Z values, the α_4 subunit actually has more ionic residues overall than α_1 (n =16 versus 14).

Looking more closely at the superfamily as a whole, it is clear that loop 2 carries the most negative charge per residue, followed by loop 7. The largest net positive charge is associated with pre-M1. The total number of charges (N) is slightly larger for the inhibitory channels (average of 11.8 versus 10.7). The "additional charge" is usually cationic, as the net charge is slightly more positive for the inhibitory channels (-1.1 versus -1.9).

We propose that Cys-loop receptors can function as long as the essential features of the electrostatic network are intact. Herein we present results concerning our study of the residues in the short, highly charged loop 2 of the nAChR α_1 subunit. As shown below, mutations that alter the charge balance are often well tolerated, apparently because they can be absorbed by the larger collection of charges. In fact, full charge reversals are quite acceptable. It appears that the essential criteria for maintaining channel function is

to conserve the number of charges in the gating interface, rather than any specific interaction involving loop 2 residues.

2.2.2 Mutations in loop 2 of the nAChR α_1 subunit

We have evaluated three residues, D44, E45, and V46, in loop 2 of the nAChR α_1 subunit.[21] These studies are both complementary to other studies in the nAChR[22] and parallel to those in other receptors,[14-16] though conservation is not strong across the superfamily. We studied the embryonic mouse muscle nAChR with a subunit composition of $(\alpha_1)_2\beta_1\delta\gamma$. This receptor shows extremely high homology with and is thus directly comparable to the *Torpedo* receptor modeled by 2BG9. We report the results of two-electrode voltage clamp determinations of EC_{50}, a measure of channel function reflecting contributions from agonist binding and gating. These residues are distinct from the agonist-binding site and therefore seem unlikely to contribute directly to binding. Furthermore, we show that representative mutations in the gating interface alter the relative efficacy of succinylcholine, a partial agonist of the receptor.[23] Extensive mutagenesis studies of loop 2 residues by Auerbach and co-workers[22] demonstrate that these residues contribute to channel gating rather than binding events. As such, we conclude that shifts in EC_{50} for the mutations reported here reflect alterations in channel gating behavior.

The loop 2 residues are DEVNQI. The neutral residues have been extensively studied by others,[22] thus we focused our efforts on the charged residues D44 and E45, and on V46, which is the loop 2 residue closest to the cell membrane in the 2BG9 structure and thus seems most likely to interact with the transmembrane domain. D44 is conserved in nicotinic α subunits and this position is generally a polar residue in other

nicotinic subunits as well as in other receptors. Charge neutralization (N) and charge reversal (K) lowered EC_{50} slightly, suggesting these mutations are well tolerated (Table 2.3).

Table 2.3 Mutations in loop 2 nAChR α_1 subunit

Mutant	EC_{50} (μM)	n_H	Mutant	EC_{50} (μM)	n_H
Wild Type	50 ± 2	1.6 ± 0.1	V46A	>1000	
D44K	14.3 ± 0.6	1.4 ± 0.1	V46I	59 ± 7	1.1 ± 0.1
D44N	20 ± 4	0.80 ± 0.08	V46T	>1000	
E45A	210 ± 20	1.1 ± 0.1	V46K	0.94 ± 0.07	1.5 ± 0.1
E45W	117 ± 7	1.3 ± 0.1	V46R	120 ± 10	1.4 ± 0.1
E45V	49 ± 4	1.9 ± 0.2	V46D	>1000	
E45D	19.2 ± 0.5	1.4 ± 0.1	V46E	>1000	
E45N	6.3 ± 0.1	1.4 ± 0.1	E45K/V46D	>1000	
E45K	6.5 ± 0.3	1.4 ± 0.1	E45K/V46E	>1000	
E45Q	1.9 ± 0.1	1.3 ± 0.1	E45R/V46D	N.E.	
E45R	1.6 ± 0.1	1.0 ± 0.1	E45R/V46E	N.E.	

The abbreviations used are as follows, N.E. = no expression as determined by radiolabelled bungarotoxin binding. EC_{50} > 1000 μM indicates sufficient surface expression and current to determine EC_{50} but that saturation had not been achieved with application of 1000 μM Ach.

Glutamate 45 (E45) is very highly conserved as an anionic (D or E) residue across the superfamily. Quite surprisingly, we find that full charge reversal (E45K or E45R) substantially lowers EC_{50} (Table 2.3), as does substitution by a neutral but polar residue (E45Q or E45N). Conversion to a hydrophobic residue (E45V) gives a wild type EC_{50}, while incorporation of a bulkier hydrophobic side chain (E45W) or reduction in the size of the side chain (E45A) result in only small increases in EC_{50}. There is no correlation between the side chain volume or hydrophobicity of the mutations at E45 (Figure 2.2).

Although the next residue in loop 2 is a neutral residue, V46, we made mutations here as well for the following reasons: (1) a proposal[8-11] based on the 2BG9 structure indicates that the V46 side chain interacts with the M2-M3 linker and is crucial to communication between the extracellular and transmembrane domains, and (2) the

surprising effect of charge reversal and charge neutralization at the preceding two residues caused us to wonder what the effects of introducing a charged side chain at V46 would be. The proposed interaction between the V46 side chain and the M2-M3 linker is discussed in depth in Chapter 4. In the present chapter we will restrict our presentation of results and discussion to the conventional mutations in Table 2.3.

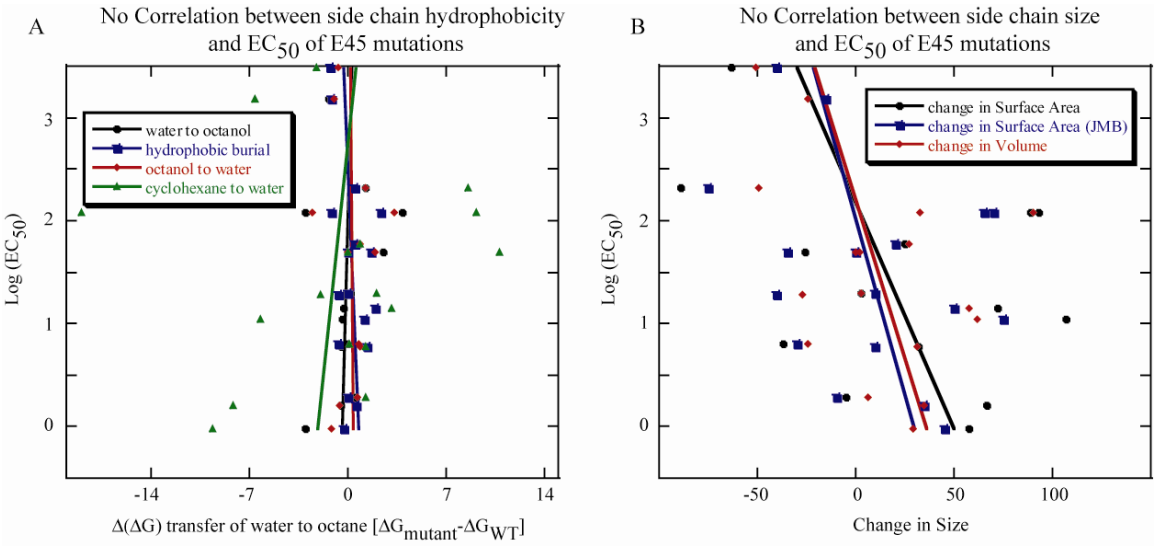

Figure 2.2 Shifts in EC_{50} of E45 mutations are not correlated with changes in side chain hydrophobitiy (**A**) or size (**B**). Four hydrophobicity scales (**A**) were used giving R=0.10 for transfer from water to octanol; 0.26 for hydrophobic burial; 0.03 for transfer from octanol to water; and 0.01 for transfer from cyclohexane to water. Three measures of size (**B**) give R=0.38, and 0.32 for surface area, respectively, and R=0.40 for volume measurements.

We reasoned that if interaction (1) is true, mutation to alanine should be highly deleterious to channel function, as was the case. Furthermore, we predicted that mutation to isoleucine would be essentially wild type, and that mutation to threonine, which is isosteric to valine, would affect EC_{50} only if the hydrophobicity of the side chain were important. The results validate our predictions and indicate that the hydrophobicity of the V46 side chain may be important, as mutation to threonine significantly impaired receptor function.

Given these results, it is surprising that introduction of a positively charged side chain (V46R) has little effect on EC_{50} or (V46K) lowers the EC_{50} ~50 fold. Conversely, introduction of a negatively charged side chain (V46D and V46E) results in a large shift in EC_{50} that cannot be measured. Attempts to rescue the effects of V46D and V46E by coupling with an EC_{50} lowering mutation at E45 (E45R or E45K) failed, and in the case of E45R resulted in loss of surface expression.

N47 in loop 2 of the nAChR α_1 subunit aligns with D57 in the $GABA_A$ α_1 subunit, which has been proposed to experience important electrostatic interactions in the $GABA_AR$.[16] Auerbach and co-workers[22] found that N47K shows a decrease in EC_{50} values while N47D shows an increase. Therefore at four consecutive residues in loop 2, introduction of a positive charge lowers the EC_{50}. Additionally, at the two neutral residues, V46 and N47, introduction of a negative charge has the opposite effect. These various side chains point in quite different directions in 2BG9. Although it is possible that all these side chains make specific electrostatic contacts that are being modulated in similar ways by the mutations introduced, it is far more likely that the global charge of loop 2, not a specific interaction, is essential to proper receptor function.

2.2.3 Studies of a Partial Agonist

To support our contention that mutations at the gating interface perturb the gating of the receptor rather than the agonist-binding site, we measured the relative efficacy (ε) of succinylcholine (SuCh), an nAChR partial agonist,[23] for wild type receptor as well as for several representative mutants. The relative efficacy is defined as the ratio of the maximal current elicited by the partial agonist to the maximal current elicited by a full agonist (ACh) (Equation 2.1). Equation 2.2 shows a highly simplified model of the

agonist binding and receptor gating processes, where R is receptor; c is closed; o is open; A is agonist; and β and α are the opening and closing rate constants, respectively. At saturating doses of agonist, all the receptors are forced into a di-liganded state (RA_2), so differences in I_{max} for the two agonists are due to differences in P_{open}. As such, ε reflects the ratio of P_{open} (the open channel probability) values for the partial and full agonists (Equation 2.1). Changes in P_{open} for an agonist are dependent only on changes in the gating rate constants (Equation 2.3). If a mutation has not altered the gating, but only the ligand binding of the receptor, the relative efficacies should be identical for the wild type and mutant receptors.[15,24]

$$\varepsilon = \frac{I_{max,PA}}{I_{max,FA}} = \frac{P_{open,PA}}{P_{open,FA}} \qquad \textbf{Equation 2.1}$$

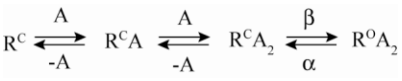

Equation 2.2

$$P_{open} = \frac{\beta}{\alpha + \beta} \qquad \textbf{Equation 2.3}$$

For the wild type nAChR, P_{open} for ACh is very nearly 1 but P_{open} for succinylcholine is only 7.5% that for acetylcholine (ε = 0.075). As a control, we examined a previously studied mutant known to affect gating. Mutation of a universally conserved leucine at the 9' position of M2 to a more polar residue such as serine (βL251S) substantially reduces EC_{50} values.[24-26] This residue forms part of the hydrophobic gate of the channel and is quite remote from the agonist-binding site, establishing it as a gating residue. As shown in Figure 2.3, the SuCh ε of the βL251S mutant is substantially increased over that of wild type. This indicates that P_{open} for SuCh has increased in the mutant, as expected for a mutation that substantially affects gating. In the α subunit, the loop 2 mutations E45R and E45Q decrease EC_{50} more than 25-fold.

All three mutations greatly increase ε, for SuCH, giving values near 1 (Figure 2.3). This indicates that these mutations ease receptor opening, allowing SuCh to act as a full agonist. More importantly, the mutation E45V, which has no affect on EC_{50}, does not alter the ε of SuCh.

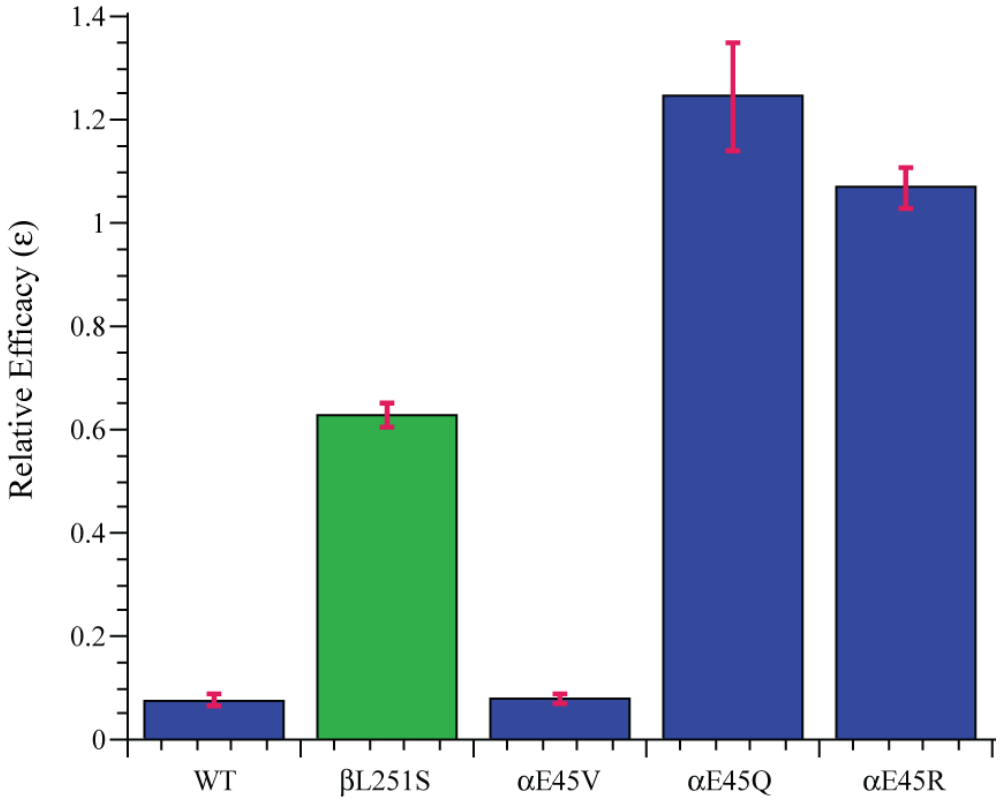

Figure 2.3 Relative efficacy of succinylcholine for representative mutations. Mutations that lower EC_{50} by affecting gating (βL251S, αE45Q, and αE45R) substantially increase the relative efficacy (ε).

2.3 Discussion

We have defined for the Cys-loop superfamily of receptors a gating interface that is composed of segments from the extracellular domain and the transmembrane domain that can reasonably be assumed to be juxtaposed, based on mutagenesis data and the best available structural information. Analysis of representative subunits from the superfamily indicates that there are a large number of ionic residues in the interface, but

for the most part their precise locations and particular charges are not conserved. Many workers, including ourselves, have sought specific ion pair interactions that exert precise control over the gating process. However, we have come to believe that, with such a large number of charges clustered in a fairly compact region, it is not meaningful to isolate specific ion pairs. Rather, the global charging pattern of the gating interface is what controls gating. Receptors have evolved to create a compatible collection of charged residues that allow the receptor to assemble and also facilitates the existence of and interconversions among multiple states.

In the current work we have presented data on charge reversal, charge neutralization, and charge introduction at three loop 2 residues. Similar mutations in other regions of the gating interface of nAChR α_1 are shown in Table 2.4.[*] Although specific ionic residues are generally not conserved, overall charging patterns are. Within the gating interface the extracellular component carries a net negative charge, and the transmembrane component carries a net positive charge. This creates a global electrostatic attraction at the interface that maintains the integrity of the receptor as it transitions from the mostly β-sheet, relatively polar extracellular domain to the α-helical, nonpolar transmembrane domain.

Several lines of evidence support this way of thinking about the gating interface. Typically, charge reversals are considered to be dramatic mutations, and they might be expected to disrupt a functionally important interface. However, one of the more remarkable features of the mutagenesis data of Tables 2.3 and 2.4 is the tolerance of the gating region to such charge disruptions. In fact, very often the EC_{50} value is *lowered* by

[*] These data were collected by Xinan Xiu and are presented here for the purpose of discussion of a global electrostatic gating interface.

such strong perturbations. It seems implausible that such dramatic mutations involving the introduction or reversal of charge just happen to lead to a viable ion pair that is tolerated by the receptor. Rather, we believe the entire gating interface is tolerant of charge up to a threshold. By distributing a large number of charges across an interface, it is possible to have movement along that interface without creating adverse situations of like charges interacting strongly or a single charge in isolation in a poorly solvated environment.

Table 2.4 Mutations in loop 7, loop 9, pre-M1, M2-M3 linker, and post M4 nAChR α_1 subunit

Mutant	EC_{50} (μM)	n_H	Mutant	EC_{50} (μM)	n_H
Wild type	50 ± 2	1.6	S266K	62 ± 6	1.54
D138A	NF		T267A	36 ± 5	1.94
D138R	NF		T267D	24 ± 2	1.21
D138K	NF		T267K	26 ± 2	1.35
D138S	NF		S268D	0.59 ± 0.02	1.82
D138N	NF		S268E	0.18 ± 0.01	1.56
D138E	28 ± 2	1.45	S268K	7.5 ± 1	1.36
D138K/K276D	66 ± 10	1.01	S269D	12 ± 0.5	1.56
D138K/R429D	50 ± 3	1.45	S269E	0.08 ± 0.01	1.34
D138R/R429E	LE		S269K	9 ± 0.6	1.22
D138E/R429K	63 ± 9		R209A	NE	
D138K/K276D/R429D	67 ± 10		R209D	NF	
K276D	45 ± 6	1.39	R209E	NF	
K276E	38 ± 2	1.28	R209K	18 ± 1	1.66
K276D/R429D	51 ± 3	1.52	D138K/R209D	NF	
R429D	57 ± 5	1.46	D138R/R209D	NS	
R429E	69 ± 5	1.29	E175R	120 ± 7	1.35
R429K	83 ± 4	1.48	E175R/R209E	NS	
R429A	90 ± 4	1.48			

The abbreviations used are as follows: NF, nonfunctional, no response to applied ACh but surface expression of receptor confirmed by α-bungarotoxin binding; L.E., functional, response to applied ACh are seen but are too weak to obtain EC_{50}; NS, no signal, no response to applied ACh, surface expression not independently verified; NE, no expression as determined by lack of α-bungarotoxin binding.

Across the superfamily, loop 2 always carries a net negative charge. When another negative charge is introduced, as in V46D, V46E, or N47D,[22] receptor function is hindered, suggesting there is an excess of negative charge in the region. In contrast,

introduction of a positive charge at the same sites, thereby decreasing the net charge of loop 2 from -2 to -1, improves (V46K, N47K) or barely impacts (V46R) receptor function. Overall these changes decrease the average extracellular charge from -3.9 to -2.9, which is still a higher magnitude charge than the positive charge of the transmembrane domain. Charge neutralization at D44 and E45 (D44N and E45Q, respectively) has the same overall effect on the region and produces a similar result of lowering the EC_{50}. Charge reversal at D44 and E45 changes the loop 2 charging pattern in the nACh α_1 subunit to a net charge of zero, yet this change is well tolerated, likely because the extracellular domain still carries a net negative charge. It thus appears that the native negative charge stabilizes the closed state of the nicotinic receptor by interacting with a positive region.

A few charge reversals in the gating interface have been shown to be deleterious, and they can often be rescued by compensating charge reversals. For example, the universally conserved D138 is one such residue. In the nAChR α_1, the $GABA_A$ α_1[16] (where it is D149) and $GABA_A$ β_2[15] (where it is D146) compensating charge reversals can rescue the initial mutant (pairwise interactions *1, 2, 4,* and *5* in Figure 2.1, A). However, the systems use completely different residues from apparently very different regions of the interface. There is certainly no universal pattern, and it appears that rather than conserving some specific pairwise interaction, it is the global charging pattern of the trio of residues that is most important. At another site, D139 of $GABA_A$ β_2[15] (I131 of nAChR α_1), as many as five different sites can contribute to compensating a charge reversal, with a gradation of efficiencies.

We conclude that no one ion pair interaction is crucially important to receptor gating across the entire Cys-loop superfamily; clearly each receptor is different. However, it may be that there is a consistent mechanism across the superfamily, but one that does not single out any particular ion pair. Several groups have suggested that the extracellular domain and the transmembrane domain change relative positions going from the closed to the open state. Harrison and co-workers[16] propose that a residue on loop 7 moves closer to a residue on M2–M3 in the $GABA_A$ receptor α_1 subunit (D149 and K279, $GABA_A$ numbering; pairwise interaction 4 in Figure 2.1, A). The detailed gating model from Unwin[11] emphasizes differential interactions between loops 2/7 (extracellular domain) and M2–M3 (transmembrane domain) along the gating pathway. We have proposed recently[13] that loop 2 and especially loop 7 interact with a specific proline on M2–M3 differentially in the open and closed states. In order to accommodate the structural rearrangement at the gating interface, the many charges involved must be comfortable in the environments provided by both the open and closed states as well as avoid any highly adverse interactions in the transition state separating the two. With a large number of charges distributed throughout the interface, the extracellular domain and the transmembrane domain can slide past one another (or twist or turn or unclamp . . .) while maintaining an acceptable network of compensating charges throughout the process. During the movement, some ion pair interactions will strengthen and some will weaken, but crucial on/off interactions seem less critical. There are clearly many ways to achieve the proper balance, and each system has evolved an ionic array that supports the desired gating behavior. The essential mechanism is universal across the Cys-loop superfamily, but the precise details vary from system to system.

2.4 Materials and Methods

Mutagenesis and mRNA Synthesis: The mRNA that codes for the muscle type nAChR subunits (α, β, δ, and γ) was obtained by linearization of the expression vector (pAMV) with NotI (Roche), followed by *in vitro* transcription using the mMessage mMachine kit purchased from Ambion (Austin, TX). The mutations in all subunits were made following the QuickChange mutagenesis protocol (Stratagene).

Electrophysiology and Data Analysis: mRNAs of α, β, δ, and γ subunits were mixed in the ratio of 2:1:1:1 and microinjected into stage VI oocytes of *Xenopus laevis*. Electrophysiology recordings were performed 24–48 h after injection in two-electrode voltage clamp mode using the OpusXpress 6000A (Axon Instruments, Molecular Devices). The holding potential was -60 mV and agonist was applied for 15 seconds.[27] Acetylcholine chloride and succinylcholine chloride dihydrate were purchased from Sigma. All drugs were diluted to the desired concentrations with calcium-free ND96 buffer. Dose-response data were obtained for at least eight concentrations of agonists and for a minimum of five oocytes. Mutants with I_{max} equal to or greater than 100 nA were defined as functional. EC_{50} and Hill coefficients (n) were calculated by fitting the dose-response relation to the Hill equation (Equation 2.4). All data are reported as mean ± standard error.

$$I = \frac{I_{\max}}{1 + EC_{50}/[A]^n} \qquad \textbf{Equation 2.4}$$

If saturation was not reached at 1000 μM concentrations of acetylcholine, the EC_{50} value could not be calculated. For two mutations, αV46A and αV46T, a second mutation was incorporated at the 9' position of the β subunit (βL251S). This mutation is

known to reduce the wild type EC_{50} to 1.2 μM.[25] The EC_{50} of the double mutant was then determined as described. For scatter plots the EC_{50} value of the double mutant was multiplied by 41.7 (50/1.2) to get a corrected EC_{50} value. The corrected EC_{50} value was used for the linear regression analysis.

EC_{50} values for succinylcholine were measured in the same manner. Maximal currents elicited by acetylcholine, $I_{max(acetylcholine)}$, and by succinylcholine, $I_{max(succinylcholine)}$, were measured sequentially at saturating concentrations on the same cell. The ratio of maximal current of succinylcholine to acetylcholine ($I_{max(succinylcholine)}/I_{max(acetylcholine)}$) was calculated for each cell and is reported as the mean ± standard error.

Bungarotoxin Binding: 48–72 hours after injection, oocytes were prewashed with calcium-free ND96 buffer with 1 mg/ml bovine serum albumin, then transferred to the same buffer with the addition of 10 nM ^{125}I-α-bungarotoxin (PerkinElmer Life Sciences), and incubated for 1 h at room temperature.[28] Oocytes were then washed four times and counted individually in a gamma counter. Oocytes injected with 50 nl of water were used to determine background. Mutants with more than five times the background reading are regarded to have sufficient expression.

2.6 References

(1) Leite, J. F.; Rodrigues-Pinguet, N.; Lester, H. A. *J Clin Invest* **2003**, *111*, 436-7.
(2) Paterson, D.; Nordberg, A. *Prog Neurobiol* **2000**, *61*, 75-111.
(3) Changeux, J.; Edelstein, S. J. *Curr Opin Neurobiol* **2001**, *11*, 369-77.
(4) Lester, H. A.; Dibas, M. I.; Dahan, D. S.; Leite, J. F.; Dougherty, D. A. *Trends Neurosci* **2004**, *27*, 329-36.
(5) Brejc, K.; van Dijk, W. J.; Klaassen, R. V.; Schuurmans, M.; van Der Oost, J.; Smit, A. B.; Sixma, T. K. *Nature* **2001**, *411*, 269-76.
(6) Celie, P. H.; Klaassen, R. V.; van Rossum-Fikkert, S. E.; van Elk, R.; van Nierop, P.; Smit, A. B.; Sixma, T. K. *J Biol Chem* **2005**, *280*, 26457-66.
(7) Celie, P. H.; van Rossum-Fikkert, S. E.; van Dijk, W. J.; Brejc, K.; Smit, A. B.; Sixma, T. K. *Neuron* **2004**, *41*, 907-14.
(8) Miyazawa, A.; Fujiyoshi, Y.; Unwin, N. *Nature* **2003**, *423*, 949-55.
(9) Unwin, N. *Novartis Found Symp* **2002**, *245*, 5-15; discussion 15-21, 165-8.
(10) Unwin, N. *FEBS Lett* **2003**, *555*, 91-5.
(11) Unwin, N. *J Mol Biol* **2005**, *346*, 967-89.
(12) Taly, A.; Delarue, M.; Grutter, T.; Nilges, M.; Le Novere, N.; Corringer, P. J.; Changeux, J. P. *Biophys J* **2005**, *88*, 3954-65.
(13) Lummis, S. C.; Beene, D. L.; Lee, L. W.; Lester, H. A.; Broadhurst, R. W.; Dougherty, D. A. *Nature* **2005**, *438*, 248-52.
(14) Kash, T. L.; Kim, T.; Trudell, J. R.; Harrison, N. L. *Neurosci Lett* **2004**, *371*, 230-4.
(15) Kash, T. L.; Dizon, M. J.; Trudell, J. R.; Harrison, N. L. *J Biol Chem* **2004**, *279*, 4887-93.
(16) Kash, T. L.; Jenkins, A.; Kelley, J. C.; Trudell, J. R.; Harrison, N. L. *Nature* **2003**, *421*, 272-5.
(17) Absalom, N. L.; Lewis, T. M.; Kaplan, W.; Pierce, K. D.; Schofield, P. R. *J Biol Chem* **2003**, *278*, 50151-7.
(18) Kash, T. L.; Trudell, J. R.; Harrison, N. L. *Biochem Soc Trans* **2004**, *32*, 540-6.
(19) Schofield, C. M.; Jenkins, A.; Harrison, N. L. *J Biol Chem* **2003**, *278*, 34079-83.
(20) Schofield, C. M.; Trudell, J. R.; Harrison, N. L. *Biochemistry* **2004**, *43*, 10058-63.
(21) Xiu, X.; Hanek, A. P.; Wang, J.; Lester, H. A.; Dougherty, D. A. *J Biol Chem* **2005**, *280*, 41655-66.
(22) Chakrapani, S.; Bailey, T. D.; Auerbach, A. *J Gen Physiol* **2004**, *123*, 341-56.
(23) Placzek, A. N.; Grassi, F.; Papke, T.; Meyer, E. M.; Papke, R. L. *Mol Pharmacol* **2004**, *66*, 169-77.
(24) Filatov, G. N.; White, M. M. *Mol Pharmacol* **1995**, *48*, 379-84.
(25) Kearney, P. C.; Zhang, H.; Zhong, W.; Dougherty, D. A.; Lester, H. A. *Neuron* **1996**, *17*, 1221-9.
(26) Labarca, C.; Nowak, M. W.; Zhang, H.; Tang, L.; Deshpande, P.; Lester, H. A. *Nature* **1995**, *376*, 514-6.
(27) Cashin, A. L.; Petersson, E. J.; Lester, H. A.; Dougherty, D. A. *J Am Chem Soc* **2005**, *127*, 350-6.
(28) Yoshii, K.; Yu, L.; Mayne, K. M.; Davidson, N.; Lester, H. A. *J Gen Physiol* **1987**, *90*, 553-73.